Molecular Pharmacology Fast Forward. Published on November 5, 2004 as doi:10.1124/mol.104.000778

MOL Manuscript #778

Membrane Structure Modulation, PKCα Activation and Anti-Cancer Activity of Minerval

Jordi Martínez, Oliver Vögler, Jesús Casas, Francisca Barceló, Regina Alemany, Jesús Prades, Tünde Nagy, Carmela Baamonde, Philip G. Kasprzyk, Silvia Terés, Carlos Saus & Pablo V. Escribá

Laboratory of Molecular and Cellular Biomedicine, Associate Unit of the Instituto de la Grasa (CSIC), Department of Biology, IUNICS, University of the Balearic Islands, Ctra. Valldemossa km 7.5, E-07122 Palma de Mallorca, Spain (J.M., O.V., J.C., F.B., R.A., J.P., T.N., C.B., S.T., C.S., P.V.E.) and Biomeasure Inc., Milford, Massachussets 01757, USA (P.G.K.)

Molecular Pharmacology Fast Forward. Published on November 5, 2004 as DOI: 10.1124/mol.104.000778
This article has not been copyedited and formatted. The final version may differ from this version.

Running Title: Anti-cancer activity of Minerval.

Corresponding authour: Pablo V. Escribá, Laboratory of Molecular and Cellular Biomedicine, Department of Biology, IUNICS, University of the Balearic Islands, Ctra. de Valldemossa km 7,5, E-07122 Palma de Mallorca, Spain. Tel.: +34 971 173433, FAX: +34 971 173184; E-mail: pablo.escriba@uib.es

Text pages: 21 without references and title/running title pages; 29 with references

Number of Tables: 0

Number of Figures: 5

Number of References: 57

Number of words in the Abstract: 221

Number of words in the Introduction: 521

ABBREVIATIONS: cdk, cyclin-dependent kinase; DNM, daunomycin; HMBA, hexamethylene bisacetamide; Minerval, 2-hydroxy-9-*cis*-octadecenoic acid; PKC, protein kinase C; $p21^{CIP}$, 21-KDa cdk-interacting protein.

Molecular Pharmacology Fast Forward. Published on November 5, 2004 as DOI: 10.1124/mol.104.000778
This article has not been copyedited and formatted. The final version may differ from this version.

ABSTRACT

Most drugs currently used for human therapy interact with proteins, altering their activity to modulate the pathologic-cell physiology. In contrast, Minerval was designed to modify the lipid organization of the membrane. Its structure was deduced following the guidelines of the mechanism of action previously proposed by us for certain anti-tumor drugs. The anti-proliferative activity of Minerval supports the above hypothesis. This molecule augments the propensity of membrane lipids to organize into nonlamellar (hexagonal H_{II}) phases, promoting the subsequent recruitment of protein kinase C (PKC) to the cell membrane. The binding of the enzyme to membranes was marked and significantly elevated by Minerval in model (liposomes) and cell (A549) membranes and in heart membranes from animals treated with this drug. In addition, Minerval induced increased PKCα expression (mRNA and protein levels) in A549 cells. This drug also induced PKC activation, which led to a p53-independent increase in $p21^{CIP}$ expression, followed by a decrease in the cellular concentrations of cyclins A, B and D3 and cdk2. These molecular changes impaired the cell cycle progression of A549 cells. At the cellular and physiological level, administration of Minerval inhibited the growth of cancer cells and exerted anti-tumor effects in animal models of cancer without apparent histological toxicity. The present results support the potential use of Minerval and related compounds in the treatment of tumor pathologies.

Molecular Pharmacology Fast Forward. Published on November 5, 2004 as DOI: 10.1124/mol.104.000778
This article has not been copyedited and formatted. The final version may differ from this version.

Introduction

Alterations in the lipid structure of the plasma membrane can modify cell signaling events (Escriba et al., 1997). Indeed, certain anti-tumor drugs appear to act by regulating signal transduction in this way (Escribá et al., 1995; 2002). While it has been proposed that the cytotoxic effects of anthracyclines are based on a direct interaction with DNA, strong evidence has accumulated indicating that other interactions are also responsible for their pharmacological activity. First, anthracycline-agarose derivatives exert their anti-tumor activity by interacting with the plasma membrane without entering the cell (Triton and Yee, 1982). Second, anthracyclines that do not bind to DNA (e.g., N-trifluoroacetyladriamycin 14-valerate, AD 32) show even greater anti-tumor effects than their DNA-binding precursors (e.g., adriamycin) (Israel et al., 1987). Third, the plasma membrane is the first cellular target encountered by anthracyclines, and membrane phospholipids bind large amounts of these drugs, accounting for their cytotoxic properties (Escriba et al., 1990). On the other hand, we found that these drugs alter the membrane structure, affecting the bilayer propensity to organize into non-lamellar phases (Escriba et al., 1995). Moreover, this phenomenon is involved in the cellular re-localization and activity of both G proteins and protein kinase C (PKC) (Escriba et al., 1995; Giorgione et al., 1995). These proteins are crucial cell signaling components and participate in cell proliferation and differentiation, thus their modulation might be responsible for the anti-tumor activity of some drugs. In line with this hypothesis, the antineoplastic agent hexamethylene bisacetamide (HMBA) induces cell differentiation by activating PKC, and also alters the membrane lipid structure (Michaeli et al., 1992; Escriba et al., 2002).

Molecular Pharmacology Fast Forward. Published on November 5, 2004 as DOI: 10.1124/mol.104.000778
This article has not been copyedited and formatted. The final version may differ from this version.

During recent years, efforts have been made to identify potential targets for anti-tumor drugs. Several alternatives have been proposed to improve the success of chemotherapy in treating cancer, such as the development of new molecular therapeutic strategies. Albeit cell membranes themselves have not been generally considered as targets for chemotherapy, it was pointed out that they could be used to develop antineoplasic agents (Spector and Burns, 1987). It has also been suggested that PKC might be an appropriate target for anti-tumor drugs (Caponigro et al., 1997), due to the role it plays in cell proliferation. With this in mind, we have designed a molecule that fulfils both these criteria (new mechanism of action based on the modulation of the plasma membrane structure and involvement of PKC in the antineoplasic activity), **2-hydroxy-9-*cis*-octadecenoic acid (Minerval)**. This is the first report on the molecular bases of the anti-tumoral activity of this drug. Minerval was designed to alter the plasma membrane structure, regulating the occurrence of non-lamellar or hexagonal H_{II} phases. As observed for anthracyclines and HMBA (Escriba et al., 1995; Escriba et al., 2002), Minerval modulated the membrane lipid structure, producing molecular and cellular alterations that influenced cell signaling. These alterations in membrane structure provoked by Minerval regulated PKC localization and activity. These molecular events correlated with the anti-proliferative and anti-tumor activities of this compound. This lipid therapy with Minerval is a pharmacological approach that differs from conventional therapies, focused on cellular proteins, and whose potential use in the clinical treatment of cancer will be determined during the next few years.

Molecular Pharmacology Fast Forward. Published on November 5, 2004 as DOI: 10.1124/mol.104.000778
This article has not been copyedited and formatted. The final version may differ from this version.

Materials and Methods

^{31}P Nuclear Magnetic Resonance (NMR). Multilamellar lipid vesicles were prepared mixing 56 mg of bovine liver phosphatidylethanolamine (PE) with deuterated water (PE:D_2O, 15:85 w/w), in the absence or presence of Minerval (PE:Minerval, 20:1, mol/mol). The lipid suspensions were hydrated and homogenized with a pestle-type minihomogenizer (Sigma), and submitted to vortex shaking until homogeneity. The suspensions were then submitted to ten heating (60ºC) and freezing (-80ºC) cycles, and equilibrated prior to data acquisition, as previously reported (9). ^{31}P NMR measurements were made in 5-mm tubes on an Advance-300 multinuclear NMR spectrometer (Bruker Instruments). Samples were equilibrated at the assay temperatures (from 5ºC to 55ºC, with increases of 2.5ºC) for 10 min before data was acquired. ^{31}P NMR free induction decays were accumulated for 64 transients by employing a 4.4 μs, 90º radio-frequency pulse, a 24.3-kHz sweep width and 65,000 data points. The delay between transients was 2 s and the spectra were obtained by scanning from lower to higher temperatures.

X-Ray Scattering. Multilamellar lipid vesicles of dielaidoyl phosphatidylethanolamine (DEPE) (15 DEPE:85 H_2O, w/w) were prepared in 20 mM Hepes, pH 7.4, in the absence or presence of Minerval (DEPE: Minerval 20:1, mole:mole). Samples were thoroughly homogenized with a pestle-type minihomogenizer (Sigma) and vortexed until a homogeneous mixture was obtained. Lipid suspensions were submitted to three temperature cycles (heating to 70ºC and cooling to 4ºC). Then, they were immediately stored at -80ºC under argon until use. Before X-ray scattering experiments were performed, the samples were equilibrated at 4ºC for 72 hours. Small and wide-angle (SAXS and WAXS) synchrotron radiation X-ray scattering data were collected simultaneously, using the standard procedures of the

Molecular Pharmacology Fast Forward. Published on November 5, 2004 as DOI: 10.1124/mol.104.000778
This article has not been copyedited and formatted. The final version may differ from this version.

Soft Condensed Matter beamline A2 at the storage ring DORIS III of the Deutsches Elektronen-Synchrotron (DESY), Hasylab (Hamburg-Germany). The positions of the observed peaks were converted into distances, *d*, after calibration using standards with well-defined scattering patterns. Silver behenate and poly-ethylene theraphtalate were used to calibrate the SAXS and WAXS regions, respectively. Data collection, was carried out at 57ºC. Interplanar distances, d_{hkl}, were calculated according to Equation 1:

$$s = 1/d_{hkl} = (2\sin\theta)/\lambda,$$

where *s* is the scattering vector, 2θ is the scattering angle, λ (0.15 nm) is the X-ray wavelength and *hkl* are the Miller indexes of the scattering planes. For hexagonal (H_{II}) phases, the unit-cell dimension, *a*, was calculated using the following relationship $a = 2d_{10}/3^{1/2}$. This parameter (*a)* also corresponds to the diameter of the rods forming the hexagonal lattice.

PKCα Binding to Liposomes. For these experiments, vesicles containing 2% Diacylglycerol, 5% Phosphatidyl-serine and 95% DOPC (Dioleoyl phosphatidylcholine) or DOPC:DOPE (DOPE, Dioleoyl phosphatidylethanolamine; 6:4, mole:mole), in the presence or absence of 5% mole of Minerval, were prepared by dissolving the lipids in chloroform and mixing the appropriate volumes in glass vials. The solvent was removed under an argon stream and the residue was maintained in a vacuum for at least 3 hours. Subsequently, 20 mM Tris·HCl buffer, pH 7.4, containing 100 mM KCl (TK buffer) and 200 mM sucrose, was added to the lipid film and incubated at 42ºC for 1 hour with vigorous vortexing every 15 minutes. This lipid suspension (large multilamellar liposomes) was passed through a 400 nm polycarbonate membrane 11 times using a mini-extruder (Avanti Polar Lipids) to obtain monolamellar vesicles of defined and homogeneous diameter. Liposome suspensions in TK buffer were combined with another 2.5 volumes of TK buffer without sucrose and centrifuged

for 45 min at 62.000 x g and 25ºC. Finally, the pellet was resuspended in TK buffer to a final concentration of 0.6 mM of lipid phosphorus. Model membranes (300 μl) were incubated in the presence of 10 μM $CaCl_2$ and 25 ng PKCα for 30 minutes at 25ºC with agitation. PKCα bound to membranes was separated from the free enzyme by centrifugation as above. The pellet containing bound PKCα was resuspended in 25 μl of electrophoresis loading buffer (84 mM Tris·HCl buffer pH 6.8, 4% SDS, 143 mM β-mercaptoethanol, 5% glycerol, 0.01% bromophenol blue). Polyacrylamide gel electrophoresis, immunoblotting and protein quantification were performed as indicated below.

Cell culture. Human lung adenocarcinoma (A549) cells were grown in 6-well plates containing 2 ml of RPMI 1640 medium, supplemented with 10 mM Hepes, pH 7.4, 10% (v/v) fetal bovine serum, 100 units/ml Penicillin, 0,1 mg/ml Streptomycin and 0,25 μg/ml Amphotericin B. When the cells reached subconfluence (approximately 70% of confluence), Minerval (100 μM) was added to the medium for 24 h, except where indicated. Immediately after the incubation period, the cell monolayers were washed twice with PBS, cell attachment was disrupted with a rubber policeman and the cells were resuspended in the appropriate buffer (see the corresponding sections). Finally, total RNA or total protein was extracted from the cells and quantified. The number of cells was determined by two methods. Live cells were counted using the trypan blue exclusion method, while cell proliferation/viability was determined by the 3-(4,5-dimethylthiazol-2-yl)-2,5-diphenyl tetrazolium bromide (MTT) method. Both methods gave similar results. Cell number was expressed as a percentage with respect to the control (untreated) cell cultures.

Electrophoresis (SDS-PAGE), immunobloting and protein quantification. For protein extraction from cultured cells, 300 μl of 10 mM Tris·HCl buffer pH 7.4,

Molecular Pharmacology Fast Forward. Published on November 5, 2004 as DOI: 10.1124/mol.104.000778
This article has not been copyedited and formatted. The final version may differ from this version.

containing 50 mM NaCl, 1 mM $MgCl_2$, 2 mM EDTA, 1% SDS, 5 mM iodoacetamide, 1 mM PMSF was added to each tissue culture well. Cell monolayers were then scraped free with a rubber policeman and the cell suspensions were transferred to 1.5-ml eppendorf tubes before being submitted to ultrasound treatment for 10 seconds at 50 W in a Braun Labsonic U sonicator. Aliquots of 30 μl were removed for total protein quantification. Then, 30 μl of 10 x electrophoresis loading buffer (120 mM Tris·HCl pH 6.8, 4% SDS, 50% glycerol, bromophenol blue 0.1%, 10% mM β-mercaptoethanol) was added to the remaining suspension, which was then boiled for 3 minutes. Proteins were separated by electrophoresis (SDS-PAGE) on 12% polyacrylamide gels (15-well- and 1.5-mm-thick), and then transferred to nitrocellulose membranes (Schleicher & Schüell). After protein transfer, the nitrocellulose membranes were incubated for 1 hour at room temperature in a blocking solution (PBS [137 mM NaCl, 2.7 mM potassium chloride, 12 mM dibasic sodium phosphate, 1.38 mM monobasic potassium phosphate at pH 7.4] containing 5% nonfat dry milk, 0.5% bovine serum albumin and 0.1% Tween 20). Then, the membranes were incubated overnight at 4ºC in blocking solution containing the specific primary antibodies: monoclonal anti-PKCα (1:1,000 dilution), anti-$p21^{CIP}$ (1:500), anti-p53 (1:500) and anti-β-actin (1:2,000), anti-cyclin A (1:1,000), anti-cyclin B (1:1,000), anti-cyclin D3 (1:1,000) and anti-cdk2 (1:1,000) (BD Transduction Laboratories, Heidelberg, Germany). After removing the primary antibody, the membranes were washed 3 times for 10 minutes with PBS, and they were then incubated with the horseradish peroxidase-linked goat antimouse IgG secondary antibody (1:2,000 dilution; Amersham Pharmacia, UK), for 2 hours at room temperature in fresh blocking solution. Immunoreactivity was detected with the Enhanced Chemiluminescence Western Blot Detection system (ECL; Amersham Pharmacia, UK)

Molecular Pharmacology Fast Forward. Published on November 5, 2004 as DOI: 10.1124/mol.104.000778
This article has not been copyedited and formatted. The final version may differ from this version.

followed by exposure to ECL hyperfilm (Amersham Pharmacia, UK; Fig 1). Films were scanned with a resolution of 63.5 μm (400 dpi).

For protein quantification by immunoblotting, the samples to be tested were evaluated using standard curves (i.e., total protein loaded vs integrated optical density [IOD]) consisting of five points of different protein content from control cells (usually between 5 and 30 μg of protein), all loaded on the same gel. This quantification procedure was repeated four times in different gels for each experiment, and experiments were replicated at least three times so that the mean value corresponds to at least 12 measurements. A linear correlation between the amount of protein loaded on the gel and IOD values was observed. The theoretical amount of protein (P_T) loaded on the gel was obtained by interpolation of the IOD value from a test sample band in the standard curve. This value was compared with the real amount of protein (P_R) loaded onto the gel. The percent value (V) with respect to controls was calculated as $V = (P_T/P_R) \times 100$, where V = 100 for the control sample used as the standard. Alternatively, the percent change (R) with respect to control was calculated as C = V-100, where C = 0 for a control sample used as standard.

mRNA determination by QRT-PCR. Quantitative reverse transcritase-polymerase chain reactions (QRT-PCR) were used to determine the transcriptional modulation of PKCα by Minerval (100 μM, 24-hour treatment). For this purpose, total RNA was extracted from of $3x10^6$ A549 cells (human lung adenocarcinoma cells) using the RNeasy Midi Kit (QIAGEN) according to the manufacturers' instructions. The RNA concentration and purity was determined by optical density at 260 and 280 nm and by agarose gel electrophoresis.

Reverse transcription (RT) reactions were performed in a total volume of 20 μl. For this purpose, 1 μg total-RNA, 1 μl oligo dT (500 μg/ml, Invitrogen), 1 μl of 10 mM

Molecular Pharmacology Fast Forward. Published on November 5, 2004 as DOI: 10.1124/mol.104.000778
This article has not been copyedited and formatted. The final version may differ from this version.

dNTPs (Invitrogen) and H_2O to 12 μl, were mixed in a tube and heated at 65ºC for 5 minutes. The tubes were then chilled quickly on ice before 4 μl of "5x First-Strand Buffer" (Invitrogen), 2 μl 0.1 M DTT and 1 μl of "RNase OUT" (recombinant ribonuclease inhibitor, Invitrogen) was added to each tube, and they were incubated at 37ºC for 2 minutes. Finally, 1 μl (200 units) of Moloney murine leukemia virus reverse transcriptase (Invitrogen), was added to the mixture which was incubated for 50 min at 37ºC. The RT reaction was stopped by heating the tubes to 70ºC for 15 min.

PCR conditions were established using a gradient thermal cycler (Eppendorf) before quantitative PCR was carried out using the following method. Oligonucleotides for PKCα amplification were 5´- ATG GAT CAC ACT GAG AAG AGG – 3´ (forward) and 5´- TCA GCT CCG AAA CTC CAA AGG – 3´ (reverse). These primers were of identical length, GC content and calculated Tm, and amplified a 342-base pair fragment. PKCα mRNA levels were corrected by β-actin mRNA levels, in order to disregard possible experimental artefacts. For this purpose, β-actin was quantified in parallel experiments by QRT-PCR using the forward primer 5´- GCG GGA AAT CGT GCG TGA CAT T – 3´ and the reverse primer 5´- CTA CCT CAA CTT CCA TCA AAG CAC – 3´, which yielded a fragment of 231 base pairs. Real-time PCR amplifications were carried out in a LightCycler thermal cycler (Roche diagnostics), using the LightCycler-FastStart DNA Master SYBR Green I kit (Roche diagnostics). The DNA concentration was determined by SYBR Green I fluorescence. PCR reaction mixtures consisted of 1 μl of DNA master SYBR Green I mixture (containing 2.5 U of Taq polymerase), 0.8 μl of $MgCl_2$ (3 mM final concentration), 0.1 μl of each forward and reverse primers (0.1 μM final concentration) and 1 μl of cDNA template (10 ng maximum) from the RT reaction, in a final volume of 10 μl. These mixtures were denatured at 95ºC for 4 minutes prior to cycling. For quantification of PKCα levels,

Molecular Pharmacology Fast Forward. Published on November 5, 2004 as DOI: 10.1124/mol.104.000778
This article has not been copyedited and formatted. The final version may differ from this version.

samples were submitted to 50 thermal cycles consisting of 4 thermal segments: 10 s at 95ºC (denaturation), 10 s at 58ºC (annealing), 18 s at 72ºC (extension) and 1 s at 81ºC (fluorescence determination). For quantification of β-actin, samples were submitted to 40 thermal cycles of 4 segments: 5 s at 95ºC, 5 s at 48ºC, 18 s at 72ºC and 1 s at 85ºC. The specificity of PCR products was determined by analysis of the amplified-DNA melting curves and agarose gel electrophoresis.

Determination of PKC activity. Approximately 3 x 10^7 A549 cells, cultured as above, were collected in ice-cold PBS, washed twice and resuspended in 1 ml of cold sample preparation buffer (50 mM Tris·HCl at pH 7.5, 50 mM β-mercaptoethanol, 10 mM EGTA, 5 mM EDTA, 1 mM PMSF, 10 mM Benzamide). The cell suspension was sonicated and then centrifuged at 100,000 x g for 60 min at 4 ºC. The pellets and supernatants were collected separately, and they were incubated at 25ºC for 10 min in 25 mM Tris·HCl at pH 7.0, 3mM $MgCl_2$, 2 mM $CaCl_2$, 0.1 mM ATP, 50 μg/ml phosphatidylserine, 0.5 mM EDTA, 1 mM EGTA, 5 mM β-mercaptoethanol, in a total volume of 108 μl. PKC activity was determined using a Protein Kinase Assay Kit (ELISA, Medical and Biological laboratories Lted, Nagoya, Japan) that measures the phosphorylation of the peptide N-RFARKGS(P)LRQKNV-C, where S(P) indicates the serine residue phosphorylated. In other series of experiments, activity of purified PKCα was also measured. The experiments were carried out similarly as above, except that 50 ng of purified enzyme were used instead of cell extracts. PKC-mediated phosphorylation was detected using a specific biotinylated anti-phosphopeptide antibody provided by the manufacturer, which was incubated in the assay sample for 1 hour at 25ºC. After washing the unbound antibody, phosphorylated-peptide/biotinylated-antibody complexes were quantified by addition of peroxidase-conjugated streptavidin (1 hour at 25ºC) followed by substrate addition (5-minute

Molecular Pharmacology Fast Forward. Published on November 5, 2004 as DOI: 10.1124/mol.104.000778
This article has not been copyedited and formatted. The final version may differ from this version.

incubation) and O.D. reading at 492 nm. PKC-mediated phosphorylation in Minerval-treated cell fractions (soluble and particulate) was expressed as the percentage ± sem values of control values (Control = 100%) of enzyme activities.

Minerval Treatments. The protocols used in this study were revised and approved by the Ethics Committee of the University of the Balearic Islands. A-549 and U87 xenograft tumor models were established by s.c. injection of tissue culture-derived tumor cells (5 x 10^6 cells/animal on the left dorsal surface) in 6-8-week-old NCr nu/nu female athymic nude mice (National Cancer Institute, Frederick, MD). The tumor volume (mm^3) was calculated as (w^2 x l)/2, where w is the width and l is the length of the tumor, as measured with calipers. Animals were monitored until day 10 postimplantation, when tumors reached an average size of approximately 55 mm^3. The animals were randomized into groups of 6 animals, so that the average tumor volumes were approximately the same for each group at the onset of treatment. Animals were treated for 5 consecutive days (twice daily, i.p. or p.o.) with Minerval (75 and 100 mg/kg, twice daily). Tumor volumes of control (untreated) and Minerval-treated animals were measured after these treatments, as indicated above. In other series of treatments, DBA/2J x C57BL/6 (F1) mice were infected with P388 murine leukemia cells (4 x 10^5 cells per animal, i.p.). One week after infection, animals were treated with either 150 mg/kg Minerval (5 times weekly) or 3 mg/kg doxorubicin (twice monthly) or both (12 animals per group in 2 independent series of treatments). The survival of the animals was monitored during 8 weeks (Kaplan-Meier survival curves).

Statistics. Results are expressed as mean ± SEM of at least three independent experiments or 12 animals. Student's *t* test or one-way ANOVA followed by Fisher's tests was used for statistical evaluations. The level of significance was chosen as $P = 0.05$.

Molecular Pharmacology Fast Forward. Published on November 5, 2004 as DOI: 10.1124/mol.104.000778
This article has not been copyedited and formatted. The final version may differ from this version.

Results and Discussion

Regulation of lipid structure by Minerval. We studied the effects of Minerval on the lipid structure of model membranes using ^{31}P NMR and X-ray scattering. In bovine liver PE membranes, the lamellar-to-hexagonal (H_{II}) phase transition was 35ºC (Fig. 1A). Below 30ºC, the lipid was only organized into lamellar phases (peak L at -12.20 ppm) (Fig. 1A). At higher temperatures (over 45ºC), PE molecules organized only into nonlamellar H_{II} phases (peak NL2 at 5.94 ppm). The peak at 0.10 ppm (NL1) corresponded to an isotropic phase, most likely an intermediate between lamellar and hexagonal phases (Fig. 1A). The presence of Minerval induced important changes in the membrane structure. On one hand, it lowered the lamellar-to-hexagonal transition temperature about 12.5ºC ($T_H \approx 22.5$ºC). On the other hand, this transition did not involve the occurrence of other nonlamellar structures (the isotropic phase peak was not observed). These results clearly indicate that Minerval had important effects on lipid mesomorphism, favoring the formation of nonlamellar (H_{II}) lipid phases. In model DEPE membranes, Minerval also induced the formation of H_{II} phases, unequivocally defined by the x-ray scattering pattern (Fig. 1B), in agreement with the above data. PE usually is the most abundant phospholipid in the cytoplasmic leaflet of mammalian plasma membranes. It is mainly organized into lamellar structures because of the presence of other phospholipid species. However, regions rich in PE have special physical properties, such as the nonlamellar-phase propensity, which may result in negative monolayer curvature or even in transient nonlamellar phases. In this context, numerous reports show that the nonlamellar phases, or the propensity to form them, increase the binding to membranes and activity of PKC (Dawson et al., 1984; Epand et al., 1991; Escribá et al., 1995; Giorgione et al., 1995; Mosior et al., 1996; Goñi and

Alonso, 1999). In fact, diacylglycerols activate PKC not only by a direct binding to the Cys-rich C1 domain of the enzyme but also by inducing hexagonal (H_{II}) phases or increasing the nonlamellar phase propensity of membranes (Dawson et al., 1984; Goldberg et al., 1994; Epand, 1985; Epand and Bottega, 1988; Epand and Lester, 1990; Janes, 1996). In a similar fashion, Minerval and structural analogs are able to lower the temperature of the lamellar-to-hexagonal (H_{II}) phase transition of model membranes. This effect is due to the "molecular shape" of the drug: only structural analogs of Minerval (e.g., fatty acids with *cis* bonds) stabilize H_{II} phases, whereas chemical analogs with divergent structure do not (Funari et al., 2003; Barceló et al., 2004; Epand et al., 1991; Goñi and Alonso, 1999). These alterations can affect the functional properties of cells for example by influencing activity of membrane proteins .

Antiproliferative and anti-tumor effects of Minerval. Similarly as anthracyclines and HMBA, Minerval inhibited cell proliferation of A549 (human lung adenocarcinoma) cells in a concentration-dependent manner (Fig. 2A). In addition, an inverse correlation between cell proliferation and the rise of PKCα levels at increasing concentrations of Minerval was observed (Fig. 2). To determine the anti-tumorigenic activity of Minerval, the inhibition of tumor-cell proliferation provoked by this drug was evaluated in xenograft tumor models. In athymic nude female mice, Minerval produced a significant inhibition of the growth of human A549 and U87 (human malignant glioma) cancers (Fig. 3A). Reductions of about 80% in the volume of subcutaneous xenograft tumors were observed after 5 days of treatment with Minerval. In mice (DBA/2J x C57BL/6, F1) infected with murine leukemia (P388) cells, Minerval had a greater anti-tumor activity than doxorubicin, an anthracycline currently used to treat leukemias and other types of cancer in human patients (Fig. 3B). Interestingly, Minerval plus doxorubicin appeared to display more potent therapeutic effects (83.3%

survival at the end of the assay) than each drug alone (66.6% and 0% of survival rates for Minerval and doxorubicin, respectively). These results indicate that the anti-proliferative activity of this drug is not restricted to cultured cells and that it is effective in whole organisms and could be used for treatment of human tumors. An important feature of the lipid therapy with Minerval is the low toxicity of the compound. In this context, we were unable to determine the maximally tolerated dose of this drug because after treatments of 3 g/kg per day for two weeks, the animals were still alive. Histological analyses of several rat organs showed that high doses of Minerval (1.2 g/kg/day, p.o.) did not induce observable toxicity (Fig. 3C). Only in liver, intracellular vesicles were observed in hepatocytes, a typical phenomenon associated with high fat intake. However, this effect was not observed at lower doses used in this study.

Minerval mechanism of action. To determine the molecular mechanisms that underlie the anti-proliferative effects of Minerval, we first studied the possible involvement of apoptosis in the alterations leading to inhibition of cancer cell proliferation. After exposure to Minerval for 24 hours (0-150 μM), we did not observe poly(ADP-ribose) polymerase (PARP) degradation in immunoblots, caspase-3 activation in enzyme immunoassays and immunoblots, or DNA breakage as determined by agarose gel electrophoresis and flow cytometry (data not shown). These results suggested that under the experimental conditions used Minerval did not promote apoptosis in A549 cells. However, other conditions or mechanisms related to apoptosis, such as paraptosis (Sperandio et al., 2000), may operate in these cells. Therefore, in other cell types or under different physiological/experimental conditions, apoptosis or cytotoxicity should not be discarded. Alternatively, cell differentiation may justify inhibition of tumor progression after treatment with Minerval. In fact, PKC activation has been associated with differentiation of various tumor cell types (Michaeli et al.,

1992; Sun and Rotenberg, 1999). Moreover, the modulation of the membrane structure, PKC recruitment to membranes and subsequent enzyme activation, have been related to the anti-tumor effects of hexamethylene bisacetamide (Escriba et al., 1995; 2002; Giorgione et al., 1995; Michaeli et al., 1992).

An alternative to apoptosis to explain the impairment of tumor progression by Minerval is the activation of anti-proliferative signals. In this context, the levels of the antiproliferative protein $p21^{CIP}$ ($p21^{CIP1/WAF1/Pic1}$, cdk-interacting protein -CIP-, wild-type p53 activated fragment -WAF-, and p53-regulated inhibitor of cdks -Pic-) were significantly increased in A549 cells exposed to Minerval (increases of 255±22%, $P<0.001$) (Fig. 4A). Induction of p53 often results in the activation of $p21^{CIP}$ transcription (el-Deiry et al., 1993) although the latter has been shown to induce exit from the cell cycle independently of p53 (Parker et al., 1995). Here, we showed that Minerval did not alter p53 levels (increase of 7±8%, $P>0.05$) (Fig. 4A), suggesting that this protein is not involved in the induction of $p21^{CIP}$. In contrast, PKCα levels were also increased in the presence of Minerval (125±14%, $P<0.001$). Interestingly, activation of PKC can induce $p21^{CIP}$ expression in a p53-independent manner in cancer cells, leading to cell cycle arrest (Detjen et al., 2000; Zezula et al., 1997; Akashi et al., 1999; Han et al., 2001; Park et al., 2001). Moreover, it has been reported that PKC-mediated phosphorylation of $p21^{CIP}$ is associated with a reduction in the activity of certain cyclin/cdk2/$p21^{CIP}$ complexes (Kashiwagi et al., 2000). In this context, different PKC isoforms can act not only directly on $p21^{CIP}$ (Kashiwagi et al., 2000) but also through other messengers (e.g., Mek1) (Zezula et al., 1997) to activate $p21^{CIP}$. These studies show that induction of PKC can lead to activation of $p21^{CIP}$, thus initiating inactivation of cyclin/cdk complexes that finally results in exit of the cell cycle. In this work, we also showed that PKC activation by phorbol esters induced the expression of

Molecular Pharmacology Fast Forward. Published on November 5, 2004 as DOI: 10.1124/mol.104.000778
This article has not been copyedited and formatted. The final version may differ from this version.

$p21^{CIP}$ and blockade of the enzyme reversed its over-expression. The present results, along with the above studies, suggest that PKC is involved in exit of the cell cycle induced by Minerval (see below).

Short-term incubations with Minerval (15-60 minutes) also induced the translocation of PKCα to A549 cell membranes (Fig. 4B). This effect was maintained during long-term (24 h) exposure to the drug (Fig. 4B), being the increase in membrane-associated PKC accompanied by a decrease in cytosolic PKC levels (Fig 4B). Moreover, induction of binding of PKC to membranes was observed not only in A549 cell membranes, but also in cardiac cell membranes from animals treated with this Minerval (increases of 48±5%, $P<0.01$).

We also studied the effect of the membrane structure on membrane-PKC interaction and its modulation by Minerval using a model system consisting of pure membrane-forming phospholipids and the purified enzyme (Fig. 4C). Membranes containing phospholipid DOPE, which was organized into H_{II} phases under the experimental conditions used, showed a greater capacity to bind PKCα (387±56%, $P<0.001$) than membranes containing only the lamellar-forming phospholipid dioleoyl phosphatidylcholine (DOPC; Fig. 4C). DOPE and DOPC are identical in their hydrophobic core and although their polar heads are chemically similar. The choline moiety in DOPC is larger than ethanolamine in DOPE. For this reason, DOPC organizes into bilayers and DOPE into hexagonal (H_{II}) phases, at room temperature (experimental conditions). Therefore, these results indicate that the membrane structure does indeed play a pivotal role in the membrane association of PKC and its subsequent activation. Furthermore, the presence of Minerval increased PKCα binding to DOPE-containing membranes but not to membranes formed exclusively of DOPC (736±61%, $P<0.01$ and 93±12%, $P>0.05$, in the presence or absence of DOPE, respectively) (Fig. 4C). The

Molecular Pharmacology Fast Forward. Published on November 5, 2004 as DOI: 10.1124/mol.104.000778
This article has not been copyedited and formatted. The final version may differ from this version.

increase of PKC binding in vesicles containing DOPE was similar to that found in the binding of this enzyme to biological membranes (Fig. 4A). These results show the importance of the lipid structure in PKC-membrane interactions and may explain in part the anti-cancer activity of Minerval. Our results may also explain the molecular/structural basis underlying PKC activation by certain unsaturated fatty acids (e.g., oleic acid and related compounds) (Lu et al., 1996), a question that remained elusive thus far. Albeit a direct interaction between fatty acids and PKC has not been described yet, it should not be discarded the possibility that this type of molecules also interacted directly with the enzyme. However, this point requires further investigations.

PKC translocation to from cytosol to membranes is associated with activation of the enzyme (Pinton et al., 2002). Here, we found that besides PKC translocation to membranes, Minerval induced significant increases of PKC activity in membranes of Minerval-treated cells (increases of 219±17%, $P<0.01$) (Fig. 4D). This drug did not alter significantly PKC activity in the absence of membranes (purified protein) (Fig. 4D).

On the other hand, Minerval induced PKCα expression in A549 cells. In whole cells (not just membranes), PKCα protein levels were markedly and significantly higher after treatment with 100 μM Minerval (increases of 125±14%, $P<0.01$, over untreated control cells, as measured by immunoblotting). In a similar fashion, PKCα mRNA levels were found elevated (increases of 274±56%, $P<0.001$, over untreated control cells, as measured by RT-PCR, which is described in the materials and methods section). Although PKC activation by phorbol esters is followed by protein down-regulation, several reports demonstrate that, under different physiological situations, enzyme activation is paralleled by increases in the levels of the protein (e.g., Sieber et al., 1998). In this context, PKC down-regulation induced by phorbol esters is due to proteolytic degradation of the strikingly activated enzyme (Junoy et al., 2002). In turn,

Molecular Pharmacology Fast Forward. Published on November 5, 2004 as DOI: 10.1124/mol.104.000778
This article has not been copyedited and formatted. The final version may differ from this version.

moderate PKC activation would result in elevated protein levels (Pintus et al., 1999), which are not masked by proteolysis.

The binding of $p21^{CIP}$ regulates various cyclin/cdk2 complexes. The association of $p21^{CIP}$ to these complexes promotes their degradation impairing the cell cycle progression (Cayrol and Ducommun, 1998). Consistent with this sequence of events, exposure to Minerval caused the down-regulation of cyclins A, B and D3 and cdk2 in A549 cells (50-70% reductions after 24-hour incubations with 100 μM Minerval) (Fig. 4E). It has been shown that $p21^{CIP}$ is involved in cellular quiescence and cell cycle arrest/exit through inactivation and/or down-regulation of cyclins (Detjen et al., 2000; Halevy et al., 1995). Usually, cell cycle progression and exit has been associated with cyclin expression and degradation, whereas cdks are often maintained at constant levels within the cell. Nevertheless, cdk2 was also down-regulated upon exposure to Minerval. In agreement with our data, it has been reported that cell cycle arrest in C33A tumor cells is associated with a decrease of both cyclin A and cdk2 protein levels (Strobeck et al., 2000). Moreover, a similar down-regulation of cyclin A and cdk2 has been observed after cell cycle arrest of cells with damaged DNA (Walker et al., 1995). In addition, reduced cellular proliferation and increased cellular differentiation have also been associated with decreases in cdk2 expression (Belachew et al., 2002; Dobashi et al., 2000). The effects of Minerval on the levels of cyclins and cdk2 were similar to those induced by serum deprivation on these proteins (reductions between 42% and 61%, data not shown), in agreement with the suggested anti-proliferative activity of this drug. Thus, it seems likely that the changes in the levels of cyclins and cdk2, provoked by exposure to Minerval, accounted for the inhibition of A549 cell proliferation observed.

The involvement of PKC in the mechanism of action of Minerval was further investigated by inhibiting the enzyme with PKC-I, a peptide corresponding to the N-

Molecular Pharmacology Fast Forward. Published on November 5, 2004 as DOI: 10.1124/mol.104.000778
This article has not been copyedited and formatted. The final version may differ from this version.

terminal (amino acids 20-28) myristoylated pseudosubstrate sequence for PKCα and β (Ward and O'Brian, 1993). PKC inhibition prevented the over-expression of PKCα induced by Minerval and reversed its effect on $p21^{CIP}$ in A549 human lung adenocarcinoma cells (Fig. 5A). Similarly, PKC-I reversed the effect of Minerval on the levels of cyclins and cdk2 (Fig. 5B). These results suggest the involvement of PKC in activation of $p21^{CIP}$ and down-regulation of cyclins and cdk2 (Figs. 5A and 5B) and in the anti-proliferative effects mediated by the drug. Moreover, PKC activation by PMA (Phorbol Myristate Acetate) provoked the up-regulation of $p21^{CIP}$ and the down-regulation of cyclins and cdk2 (Fig. 5C). These data are in agreement with the involvement of PKCα in the pharmacological mechanism of action of Minerval leading to impairment of cell proliferation, as described for other anti-tumor drugs (Michaeli et al., 1992; Escribá et al., 2002). Also in line with the present results, it has been shown that PKC activation mediates growth inhibition of endothelial cells, which can be also reversed by PKC inhibitors (Zezula et al., 1997). In that study and in this work, PKC activation by phorbol esters induced $p21^{CIP}$ in endothelial and epithelial cells, respectively. Taken together, the present results show that PKC, $p21^{CIP}$, cyclins and cdk2 are involved in the pharmacological effects exerted by Minerval.

Lipid Therapy. The membrane lipid structure has been shown to influence cell signaling (Escribá et al., 1997; Vögler et al., 2004). The lipid composition of membranes has also been associated with the development of human pathologies (e.g., Escribá et al., 2003). The present data suggest that the anti-proliferative activity of Minerval could be related to the regulation of the membrane structure and subsequent PKC recruitment to the membrane. The hexagonal phase propensity of membranes has been associated with the interaction of several amphitropic proteins (Kinnunen, 1996). In line with this, heterotrimeric Gi proteins and Gβγ dimers prefer nonlamellar-prone

Molecular Pharmacology Fast Forward. Published on November 5, 2004 as DOI: 10.1124/mol.104.000778
This article has not been copyedited and formatted. The final version may differ from this version.

membranes whereas the Gαi monomer, formed upon agonist activation of G protein-coupled receptors, has a greater affinity for lamellar phases (Vögler et al., 2004). This differential interaction with membrane lipids drives in part the cellular localization and activity of resting (Gαβγ) and active (Gα and Gβγ) G proteins. Because G proteins and related systems are targets for a great number of marketed drugs, the modulation of these systems is of great clinical relevance. Moreover, many cell functions occur in or around membranes, so that the differential modulation of the membrane lipid structure and/or composition will probably result in the modulation of other proteins. Although the modulation of the membrane structure itself has not been considered for the development of clinical drugs, evidence has been gathered showing that compounds that alter the membrane structure regulate cellular functions. Agents such as alcohols, detergents, anesthetics, nonimmobilizers, organic solvents, surfactants and other types of molecules modulate the membrane structure with their own characteristic features (Shen et al., 1999; Koubi et al., 2001; Lester and Baumann, 1991; Perkins et al., 1996). Lipid therapy differs with other conventional therapeutic strategies in that the first target of the drug is not a protein itself, but the membrane lipids. Indeed, the potential for this approach is supported by the fact that the anti-tumor agents DNM and HMBA, which alter the cellular distribution and activity of PKC, also modulate the plasma membrane structure (Escriba et al., 1995; Giorgione et al., 1995; Escriba et al., 2002; Michaeli et al., 1992).

Due to the current view of the cell membrane as a mere support for membrane proteins, one might envisage that lipid therapy would either be an unspecific or a poorly effective treatment. Nevertheless, the expression of certain proteins is often ubiquitous or widespread in cells, and the effectiveness and specificity of many drug treatments targeting such proteins is not questioned. A wide variety of cell membranes exist,

containing different lipid species, lipid compositions, and lipid shapes. For example, the numerous organelles within a cell have different membrane types, each containing specific lipid species (Deshmukh et al., 1988). Indeed, even within an individual membrane, the exoplasmic and cytoplasmic leaflets can display quite different lipid compositions (Verkleij et al., 1973; Bloj and Zilversmit, 1976; Rothman and Lenard, 1977). Moreover, localized or mobile specialized membrane domains or membrane structures may also exist (membrane rafts, caveolae, synaptosomes, brush borders, etc) (Mañes et al., 1999; Vereb et al., 2001). This diversity and the exquisite regulation of the lipid levels, argues in favor of the possibility of designing specific lipid therapies. In fact, treatments with drugs that modulate the structure of the membrane and diets rich in certain oils that regulate the membrane lipid properties also alter the expression of some genes (Escribá et al., 2002; Puskás et al., 2003).

Despite the variety of studies that we have carried out to reveal the molecular bases of Minerval action, many questions require further investigations. In this context, other molecular mechanisms could also be involved in the anti-cancer activity of Minerval. The presence of the hydroxyl moiety on its alpha carbon may interfere with mitochondrial import of fatty acids, β-oxidation, PPARs activities, etc. These molecular entities and/or mechanisms that Minerval may modulate are currently under investigation. However, the lack of relevant toxicology and side-effects and the oral administration of Minerval, as well as its anti-proliferative and anti-tumoral activities support its potential use in clinical therapies.

Molecular Pharmacology Fast Forward. Published on November 5, 2004 as DOI: 10.1124/mol.104.000778
This article has not been copyedited and formatted. The final version may differ from this version.

REFERENCES

Akashi M, Osawa Y, Koeffler HP, and Hachiya M (1999) $p21^{WAF1}$ expression by an activator of protein kinase C is regulated mainly at the post-transcriptional level in cells lacking p53: important role of RNA stabilization. *Biochem J* **337**:607-616.

Barceló F, Prades J, Funari SS, Frau J, Alemany R, and Escribá PV (2004) The hypotensive drug 2-hydroxyoleic acid modifies the structural properties of model membranes. *Mol Membr Biol* **in press**.

Belachew S, Aguirre AA, Wang H, Vautier F, Yuan X, Anderson S, Kirby M, and Gallo V (2002) Cyclin-dependent kinase-2 controls oligodendrocyte progenitor cell cycle progression and is downregulated in adult oligodendrocyte progenitors. *J Neurosci* **22**:8553-8562.

Bloj B and Zilversmit DB (1976) Asymmetry and transposition rates of phosphatidylcholine in rat erythrocyte ghosts. *Biochemistry* **15**:1277-1283.

Caponigro F, French RC, and Kaye SB (1997) Protein kinase C: a worthwhile target for anticancer drugs? *Anticancer Drugs* **8**:26-33.

Cayrol C and Ducommun B (1998) Interaction with cyclin-dependent kinases and PCNA modulates proteasome- dependent degradation of p21. *Oncogene* **17**:2437-2444.

Dawson RM, Irvine RF, Bray J, and Quinn PJ (1984) Long-chain unsaturated diacylglycerols cause a perturbation in the structure of phospholipid bilayers rendering them susceptible to phospholipase attack. *Biochem Biophys Res Commun* **125**:836-842.

Deshmukh DS, Vorbrodt AW, Lee PK, Bear WD, and Kuizon S (1988) Studies on the submicrosomal fractions of bovine oligodendroglia: lipid composition and glycolipid biosynthesis. *Neurochem Res* **13**:571-582.

Detjen KM, Brembeck FH, Welzel M, Kaiser A, Haller H, Wiedenmann B, and Rosewicz S (2000) Activation of protein kinase Calpha inhibits growth of pancreatic cancer cells via $p21^{cip}$-mediated G_1 arrest. *J Cell Sci* **113**:3025-3035.

Dobashi Y, Shoji M, Kitagawa M, Noguchi T, and Kameya T (2000) Simultaneous suppression of cdc2 and cdk2 activities induces neuronal differentiation of PC12 cells. *J Biol Chem* **275**:12572-12580.

el-Deiry WS, Tokino T, Velculescu VE, Levy DB, Parsons R, Trent JM, Lin D, Mercer WE, Kinzler KW, and Vogelstein B (1993) WAF1, a potential mediator of p53 tumor suppression. *Cell* **75**:817-825.

Epand RM (1985) Diacylglycerols, lysolecithin or hydrocarbons markedly alter the bilayer to hexagonal phase transition temperature of phosphatidylethanolamines. *Biochemistry* **24**, 7092-7095.

Epand RM and Bottega R (1988) Determination of the phase behaviour of phosphatidylethanolamine admixed with other lipids and the effects of calcium chloride: implications for protein kinase C regulation. *Biochim Biophys Acta* **944**:144-154.

Epand RM and Lester DS (1990) The role of membrane biophysical properties in the regulation of protein kinase C activity. *Trends Pharmacol Sci* **11**:317-320.

Epand RM, Epand RF, Ahmed N, and Chen R (1991) Promotion of hexagonal phase formation and lipid mixing by fatty acids with varying degrees of unsaturation. *Chem Phys Lipids* **57**:75-80.

Escriba PV, Ferrer-Montiel AV, Ferragut JA, and Gonzalez-Ros JM (1990) Role of membrane lipids in the interaction of daunomycin with plasma membranes from tumor cells: implications in drug-resistance phenomena. *Biochemistry* **29**:7275-7282.

Escriba PV, Morales P, and Smith A (2002) Membrane phospholipid reorganization differentially regulates metallothionein and heme oxygenase by heme-hemopexin. *DNA Cell Biol* **21**:355-364.

Escriba PV, Ozaita A, Ribas C, Miralles A, Fodor E, Farkas T, and Garcia-Sevilla JA (1997) Role of lipid polymorphism in G protein-membrane interactions: nonlamellar-prone phospholipids and peripheral protein binding to membranes. *Proc Natl Acad Sci U S A* **94**:11375-11380.

Escribá PV, Sánchez-Dominguez JM, Alemany R, Perona JS, and Ruiz-Gutierrez V (2003) Alteration of lipids, G proteins and PKC in cell membranes of elderly hypertensives. *Hypertension* **41**:176-182.

Escriba PV, Sastre M, and Garcia-Sevilla JA (1995) Disruption of cellular signaling pathways by daunomycin through destabilization of nonlamellar membrane structures. *Proc Natl Acad Sci U S A* **92**:7595-7599.

Funari SS, Barcelo F, and Escriba PV (2003) Effects of oleic acid and its congeners, elaidic and stearic acids, on the structural properties of phosphatidylethanolamine membranes. *J Lipid Res* **44**:567-575.

Giorgione J, Epand RM, Buda C, and Farkas T (1995) Role of phospholipids containing docosahexaenoyl chains in modulating the activity of protein kinase C. *Proc Natl Acad Sci U S A* **92**:9767-9770.

Goldberg EM, Lester DS, Borchardt DB, and Zidovetzki R (1994) Effects of diacylglycerols and Ca^{2+} on structure of phosphatidylcholine/phosphatidyl-serine bilayers. *Biophys J* **66**:382-393.

Goñi FM and Alonso A (1999) Structure and functional properties of diacylglycerols in membranes. *Prog Lipid Res* **38**:1-48.

Halevy O, Novitch BG, Spicer DB, Skapek SX, Rhee J, Hannon GJ, Beach D, and Lassar AB (1995) Correlation of terminal cell cycle arrest of skeletal muscle with induction of p21 by MyoD. *Science* **267**:1018-1021.

Han JW, Ahn SH, Kim YK, Bae GU, Yoon JW, Hong S, Lee HY, Lee YW, and Lee HW (2001) Activation of $p21^{WAF1/Cip1}$ transcription through Sp1 sites by histone deacetylase inhibitor apicidin: involvement of protein kinase C. *J Biol Chem* **276**:42084-42090.

Israel M, Idriss JM, Koseki Y, and Khetarpal VK (1987) Comparative effects of adriamycin and DNA-non-binding analogues on DNA, RNA, and protein synthesis in vitro. *Cancer Chemother Pharmacol* **20**:277-84.

Janes N (1996) Curvature stress and polymorphism in membranes. *Chem Phys Lipids* **81**:133-150.

Junoy B, Maccario H, Mas JL, Enjalbert A, and Drouva SV (2002) Proteasome implicated in phorbol ester- and GnRH-induced selective down-regulation of PKC (α, ε, ζ) in αT_3-1 and $L\beta T_2$ gonadotrope cell lines. *Endocrinology* **143**:1386-1403.

Kashiwagi M, Ohba M, Watanabe H, Ishino K, Kasahara K, Sanai Y, Taya Y, and Kuroki T (2000) PKCε associates with cyclin E/cdk2/p21 complex, phosphorylates p21 and inhibits cdk2 kinase in keratinocytes. *Oncogene* **19**:6334-6341.

Kinnunen PKJ (1996) On the molecular-level mechanism of peripheral protein-membrane interactions induced by lipids forming inverted non-lamellar phases. *Chem Phys Lipids* **81**:151-166.

Koubi L, Tarek M, Bandyopadhyay S, Klein ML, and Scharf D (2002) Membrane structural perturbations caused by anesthetics and nonimmobilizers: a molecular dynamics investigation. *Biophys J* **81**:3339-3345.

Lester DS, and Baumann D (1991) Action of organic solvents on protein kinase C. *Eur J Pharmacol* **206**:301-308.

Lu G, Morinelli TA, Meier KE, Rosenzweig SA, and Egan BM (1996) Oleic acid-induced mitogenic signaling in vascular smooth muscle cells. A role for protein kinase C. *Circ Res* **79**:611-618.

Mañes S, Mira E, Gomez-Mouton C, Lacalle RA, Keller P, Labrador JP, and Martínez-A C (1999) Membrane raft microdomains mediate frot-rear polarity in migrating cells. *EMBO J* **18**:6211-6220.

Michaeli J, Busquets X, Orlow I, Younes A, Colomer D, Marks PA, Rifkind RA, and Kolesnick RN (1992) A rise and fall in 1,2-diacylglycerol content signal hexamethylene bisacetamide-induced erythropoiesis. *J Biol Chem* **267**:23463-23466.

Mosior M, Golini ES, and Epand RM (1996) Chemical specificity and physical properties of the bilayer in the regulation of protein kinase C by anionic phospholipids: evidence for the lack of a specific binding site for phosphatidylserine. *Proc Natl Acad Sci U S A* **93**:1907-1912.

Park JW, Jang MA, Lee YH, Passaniti A, and Kwon TK (2001) p53-independent elevation of p21 expression by PMA results from PKC-mediated mRNA stabilization. *Biochem Biophys Res Commun* **280**:244-248.

Parker SB, Eichele G, Zhang P, Rawls A, Sands AT, Bradley A, Olson EN, Harper JW and Elledge SJ (1995) p53-independent expression of $p21^{Cip1}$ in muscle and other terminally differentiating cells. *Science* **267**:1024-1027.

Perkins WR, Dause RB, Parente RA, Minchey SR, Neuman KC, Gruner SM, Taraschi TF, and Janoff AS (1996) Role of lipid polymorphism in pulmonary surfactant. *Science* **273**, 330-332.

Pinton P, Tsuboi T, Ainscow EK, Pozzan T, Rizzuto R, and Rutter GA (2002) Dynamics of glucose-induced membrane recruitment of protein kinase C βII in living pancreatic islet β-cells. *J Biol Chem* **277**:37702-37710.

Pintus G, Tandolini B, Maioli M, Posadino AM, Gaspa L, and Ventura C (1999) Heparin down-regulates the phorbol ester-induced protein kinase C gene expression in human endothelial cells: enzyme-mediated autoregulation of protein kinase C-α and -δ genes. *FEBS Letters* **449**:135-140.

Puskás LG, Kitajka K, Nyakas C, Barceló-Coblijn G, and Farkas T (2003) Short-term administration of omega 3 fatty acids from fish oil results in increased transthyretin transcription in old rat hippocampus. *Proc Natl Acad Sci U S A* **100**:1580-1585.

Rothman JE and Lenard J (1977) Membrane asymmetry. *Science* **195**:743-753.

Shen Y-M A, Chertihin OI, Biltonen RL, and Sando JJ (1999) Lipid-dependent activation of protein kinase C-α by normal alcohols. *J Biol Chem* **274**, 34036-34044.

Sieber FE, Traystman RJ, Brown PR, and Martin LJ (1998) Protein kinase C expression and activity after global incomplete cerebral ischemia in dogs. *Stroke* **29**:1445-1452.

Spector AA and Burns CP (1987) Biological and therapeutic potential of membrane lipid modification in tumors. *Cancer Res* **47**:4529-4537.

Sperandio S, de Belle I, and Bredesen DE (2000) An alternative, nonapoptotic form of programmed cell death, *Proc. Natl. Acad. Sci. U S A* **97**:14376-14381.

Strobeck MW, Fribourg AF, Puga A, and Knudsen ES (2000) Restoration of retinoblastoma mediated signaling to Cdk2 results in cell cycle arrest. *Oncogene* **19**:1857-1867.

Sun XG and Rotenberg SA (1999) Overexpression of protein kinase Cα in MCF-10A human breast cells engenders dramatic alterations in morphology, proliferation, and motility. *Cell Growth Differ* **10**:343-352.

Triton TR and Yee G (1982) The anticancer agent adriamycin can be actively cytotoxic without entering cells. *Science* **217**:248-250.

Vereb G, Szollosi J, Matko J, Nagy P, Farkas T, Vigh L, Matyus L, Waldmann TA, and Damjanovich S (2003) Dynamic, yet structured: The cell membrane three decades after the Singer-Nicolson model. *Proc Natl Acad Sci U S A* **100**:8053-8058.

Verkleij AJ, Zwaal RF, Roelofsen B, Comfurius P, Kastelijn D, and van Deenen LL (1973) The asymmetric distribution of phospholipids in the human red cell membrane. A combined study using phospholipases and freeze-etch electron microscopy. *Biochim Biophys Acta* **323**:178-193.

Vögler O, Casas J, Capó D, Nagy T, Borchert G, Martorell G, and Escribá PV (2004) The Gβγ dimer drives the interaction of heterotrimeric Gi proteins with nonlamellar membrane structures. *J Biol Chem* **6**:36540-36545.

Walker DH, Adami GR, Dold KM, and Babiss LE (1995) Misregulated expression of the cyclin dependent kinase 2 protein in human fibroblasts is accompanied by

the inability to maintain a G2 arrest following DNA damage. *Cell Growth Differ* **6**:1053-1061.

Ward NE and O'Brian CA (1993) Inhibition of protein kinase C by N-myristoylated peptide substrate analogs. *Biochemistry* **32**:11903-11909.

Zezula J, Sexl V, Hutter C, Karel A, Schutz W, and Freissmuth M (1997) The cyclin-dependent kinase inhibitor $p21^{cip1}$ mediates the growth inhibitory effect of phorbol esters in human venous endothelial cells. *J Biol Chem* **272**:29967-29974.

Molecular Pharmacology Fast Forward. Published on November 5, 2004 as DOI: 10.1124/mol.104.000778
This article has not been copyedited and formatted. The final version may differ from this version.

Footnotes

This work was supported in part by Grants FIS PI/031218 (R.A.), FIS00/1029, SAF2001-0839, SAF2003-00232, SAF2004-05249 and CAO01-002 (P.V.E.). 'Fundacion Marathon', 'Conselleria de Sanitat' and 'Conselleria d'Innovació i Tecnologia (PRDIB-2002GC2-11) del Govern Balear' also provided funds for this work (P.V.E.). Jesús Casas and Tünde Nagy were supported by fellowships from the Spanish 'Ministerio de Educación, Cultura y Deportes'. Jesús Prades was supported by a fellowship from the 'Conselleria d'Innovació i Tecnologia del Govern Balear'. Regina Alemany and Oliver Vögler are "Ramón y Cajal" fellows.

Send reprint requests to: Pablo V. Escribá, Laboratory of Molecular and Cellular Biomedicine, Department of Biology, IUNICS, University of the Balearic Islands, Ctra. de Valldemossa km 7,5, E-07122 Palma de Mallorca, Spain. Tel.: +34 971 173433, FAX: +34 971 173184; E-mail: pablo.escriba@uib.es

Molecular Pharmacology Fast Forward. Published on November 5, 2004 as DOI: 10.1124/mol.104.000778
This article has not been copyedited and formatted. The final version may differ from this version.

Legends for Figures

Figure 1. Effect of Minerval on the structure of model membranes. A, ^{31}P NMR of bovine liver PE membranes in the absence (left) or presence (right) of Minerval at different temperatures. The observed peaks corresponded to the lamellar (L), nonlamellar isotropic (NL1) and nonlamellar H_{II} (NL2) phases. B, X-ray scattering of DEPE membranes showed that Minerval induced the occurrence of non-lamellar (hexagonal H_{II}) phases. The peaks corresponding to lattice distances for lamellar (dL) and hexagonal phases (dH) are indicated.

Figure 2. Anti-proliferative activity of Minerval. A, The graph shows the effect of various concentrations of Minerval (24-h cultures) on the growth of A549 cells (solid circles). Control values correspond to untreated cells (100%, 5 x 10^5 cells/ml). Open symbols correspond to the levels of PKCα protein over control (untreated cells: 0% of increase). Results are means of 12 measurements from four independent experiments. B, The pictures show typical subconfluent cultures of control (C) and Minerval-treated (M, 100 μM) A549 cells.

Figure 3. Anti-tumor effects of Minerval. A, Effect of Minerval on xenograft tumors from A549 (human lung adenocarcinoma) and U87 (human malignant glioma) cells in nude athymic mice. Tumor volumes (mm^3) were determined before and after 5 days of treatment (days 10-14 after tumor-cell implantation). Bars correspond to mean ± sem of tumor volume increase in untreated (control) and Minerval-treated animals (75 mg/kg, M1 or 100 mg/kg, M2). B, Kaplan-Meier survival curves for mice infected with P388 murine leukemia cells. Mice (12 animals per group) were treated with saline (solid circles), doxorubicin (solid triangles), Minerval (open triangles) or Minerval plus doxorubicin (open diamonds). Survival of non-infected animals is also shown (solid

squares). C, Histological toxicity after Minerval treatments. Animals were treated with vehicle (control, C, upper panels) or Minerval (M, lower panels) (1,200 mg/kg/day, p.o., 1 week). Sections from paraformaldehyde-fixed and paraffin-embedded tissues were submitted to hematoxylin-eosin staining and photographed at a 50-100-fold magnification.

Figure 4. Minerval mechanism of action. A, Effects of Minerval treatments (100 μM, 24 hours) on the density of PKCα, $p21^{CIP}$ and p53 in A549 cells, measured by immunoblotting analysis. Bars correspond to means of 6 independent experiments. Representative immunoblots are shown on the right. **P*<0.001. B, Minerval treatments on PKCα translocation to membranes. PKCα recruitment to A549 cell membranes after 45-minute and 24-hour treatments was measured by immunoblotting. The corresponding PKCα decreases in cytosol fractions were also measured from control (untreated) and Minerval-treated A549 cells. Bars are means of 4 independent experiments. **P*<0.01. C, Binding of purified PKCα to model membranes (liposomes) of DOPC (PC) (lamellar-prone phospholipid) in the absence or presence of Minerval are shown on the left side of the graph. On the right side, PKCα binding to membranes containing DOPE (nonlamellar-prone phospholipid, DOPC:DOPE 6:4, mol:mol) (PCPE) is shown. Bars are means of 3 independent experiments. **P*<0.001 versus the corresponding PC vesicles; #*P*<0.01 versus PCPE without Minerval. D, Effect of Minerval on PKC activity. The bars correspond to enzyme activity in membrane fractions ("Membrane") from A549 cells treated with Minerval and from untreated control cells. Minerval had no significant effect on PKC activity in the absence of membranes (purified protein, "membrane-free"). Results are expressed as percent values of the corresponding control (in the absence of Minerval). Basal PKC activity in the presence of membranes was about 5-fold greater than that in a membrane-free

Molecular Pharmacology Fast Forward. Published on November 5, 2004 as DOI: 10.1124/mol.104.000778
This article has not been copyedited and formatted. The final version may differ from this version.

system. Bars are means of 3 independent experiments. **P*<0.01. E, Effect of Minerval on cyclins A, B and D3 and cdk2. A549 cells were treated during 24 h with Minerval (100 μM) and the cellular content of these proteins was quantified by immunoblotting and compared with the levels in untreated control cells (100%). Minerval treatments did not induce significant changes in the levels of β-Actin. Bars are means of at least 4 independent experiments. **P*<0.01 versus the corresponding control.

Figure 5. Role of PKC activity in the molecular mechanism of Minerval. A, Effect of the PKC inhibitor, PKC-I, on the expression of PKCα and $p21^{CIP}$. Minerval (M, 100 μM, 24 hours) induced up-regulation of PKCα and $p21^{CIP}$ in A549 cells. PKC activity was inhibited by PKC-I, reversing PKCα over-expression and inducing a down-regulation of $p21^{CIP}$ either in the presence (M+PKC-I) or absence (PKC-I) of Minerval. B, Effects of PKC inhibition on cyclin and cdk2 expression. PKCα inhibition reversed the effects of Minerval (M) on cyclin A and B and cdk2. C, PKC activation by the phorbol ester PMA induced similar effects to those induced by Minerval. **P*<0.01.

A

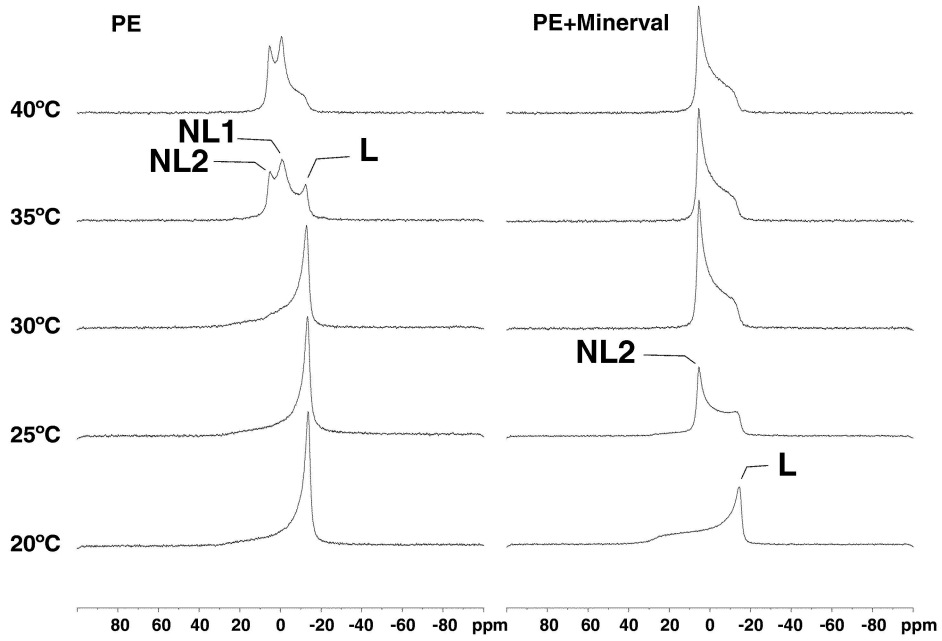
PE
PE+Minerval
40°C
35°C
30°C
25°C
20°C
NL1
NL2
L
NL2
L
80 60 40 20 0 -20 -40 -60 -80 ppm
80 60 40 20 0 -20 -40 -60 -80 ppm

B

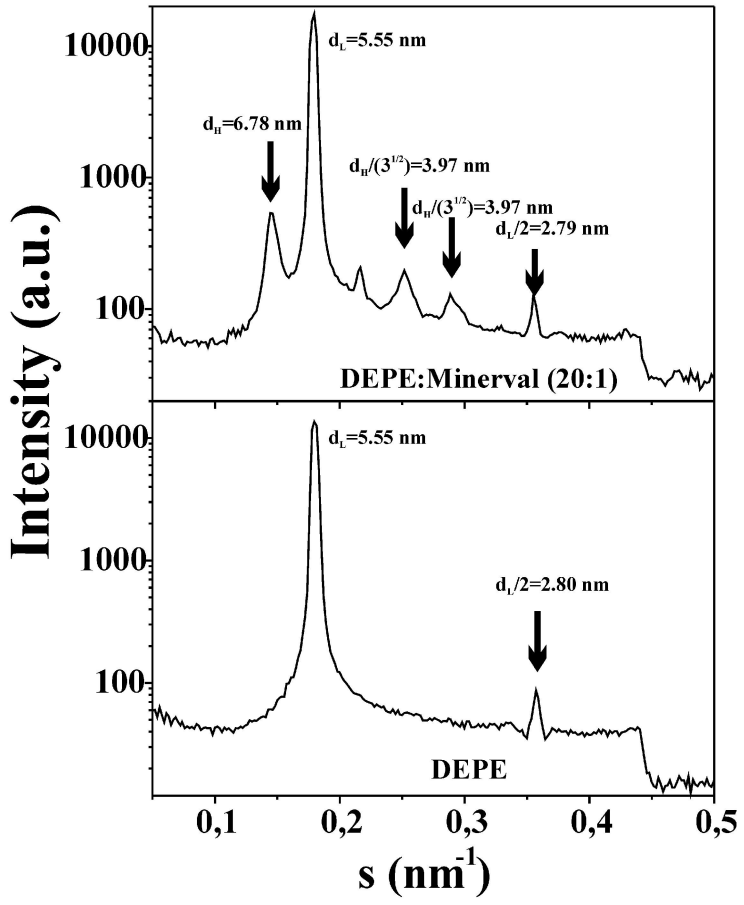
Intensity (a.u.)
10000
1000
100
d_L=5.55 nm
d_H=6.78 nm
$d_H/(3^{1/2})$=3.97 nm
$d_H/(3^{1/2})$=3.97 nm
$d_L/2$=2.79 nm
DEPE:Minerval (20:1)
10000
1000
100
d_L=5.55 nm
$d_L/2$=2.80 nm
DEPE
0,1
0,2
0,3
0,4
0,5
s (nm^{-1})

Figure 1

A

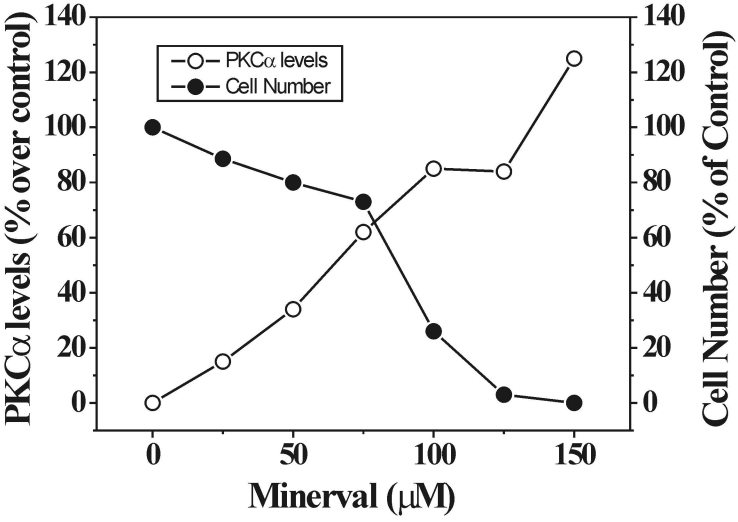
PKCα levels
Cell Number
PKCα levels (% over control)
Cell Number (% of Control)
Minerval (μM)
0
20
40
60
80
100
120
140
0
50
100
150

B

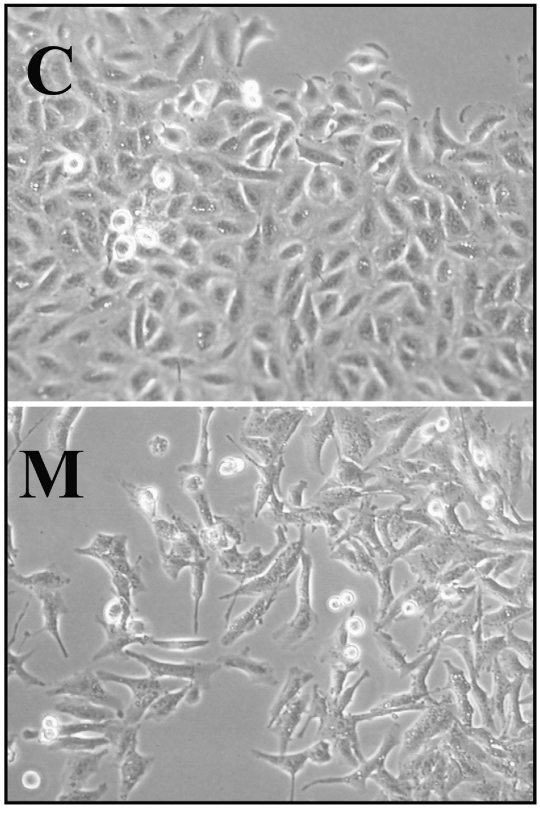
C
M

Figure 2

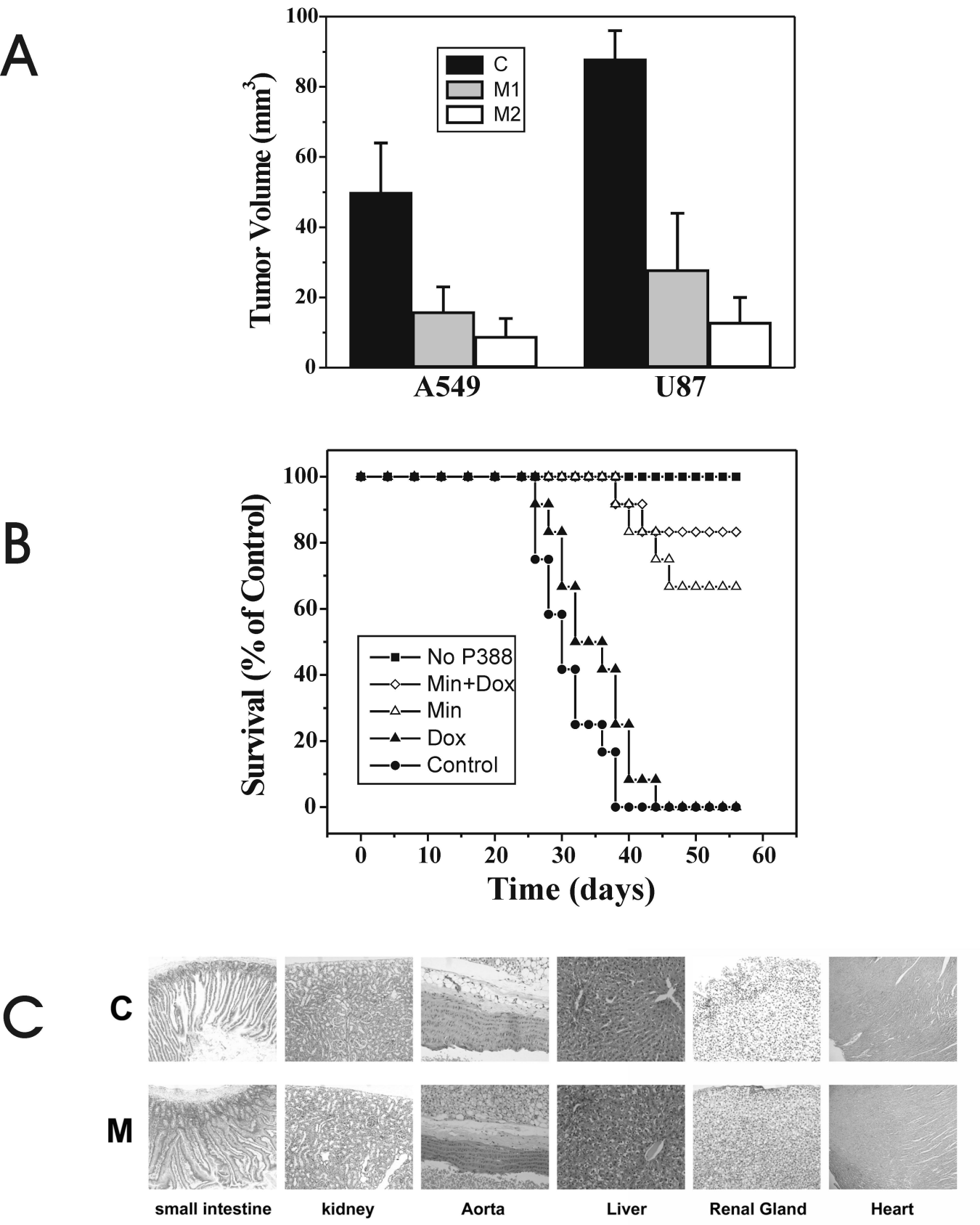
A
Tumor Volume (mm3)
C
M1
M2
A549
U87
B
Survival (% of Control)
No P388
Min+Dox
Min
Dox
Control
Time (days)
C
M
small intestine
kidney
Aorta
Liver
Renal Gland
Heart

Figure 3

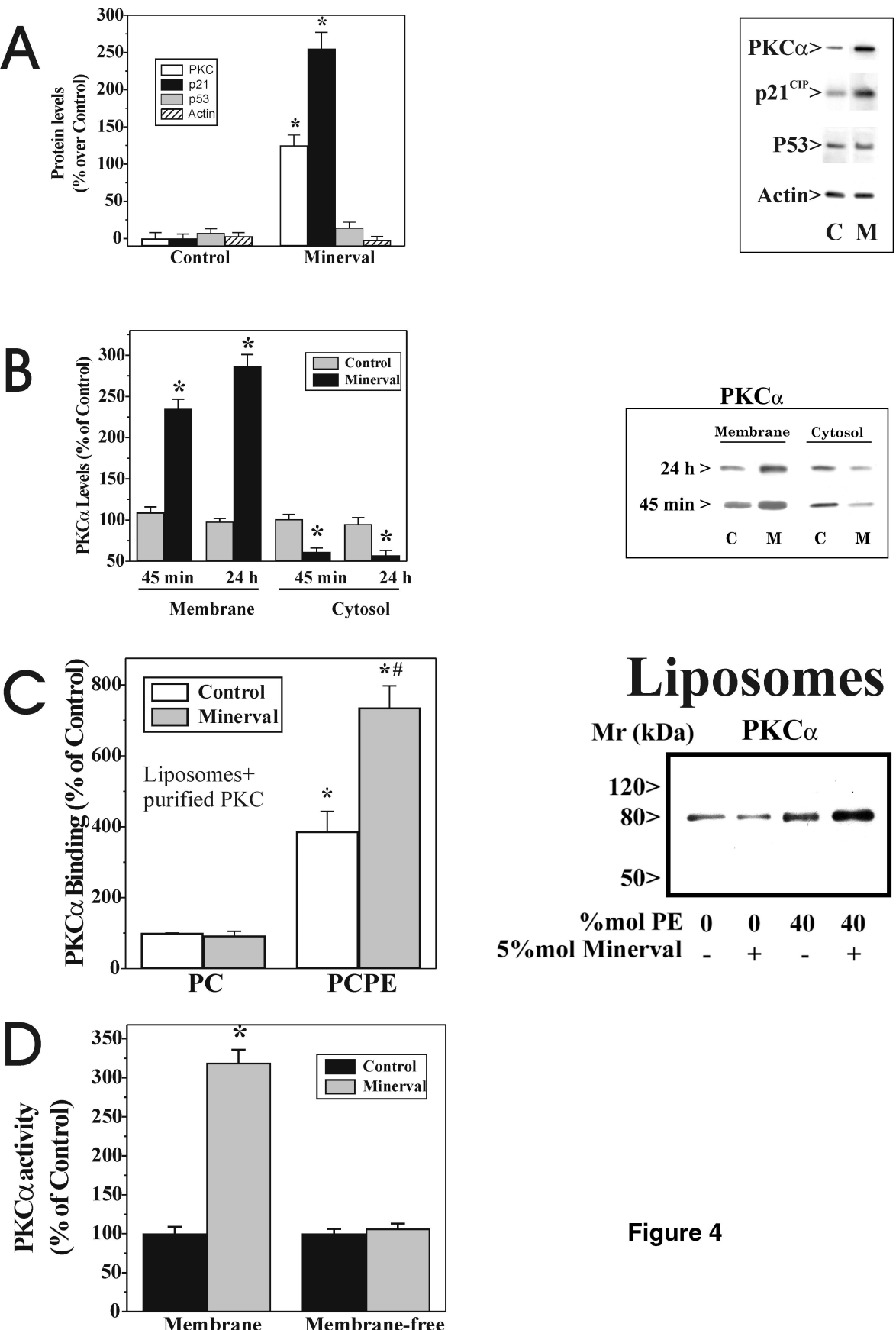
A
Protein levels (% over Control)
PKC
p21
p53
Actin
Control
Minerval
PKCα>
p21CIP>
P53>
Actin>
C M
B
PKCα Levels (% of Control)
Control
Minerval
45 min
24 h
45 min
24 h
Membrane
Cytosol
PKCα
Membrane
Cytosol
24 h >
45 min >
C M C M
C
PKCα Binding (% of Control)
Control
Minerval
Liposomes+
purified PKC
PC
PCPE
Liposomes
Mr (kDa)
PKCα
120>
80>
50>
%mol PE 0 0 40 40
5%mol Minerval - + - +
D
PKCα activity
(% of Control)
Control
Minerval
Membrane
Membrane-free

Figure 4

E

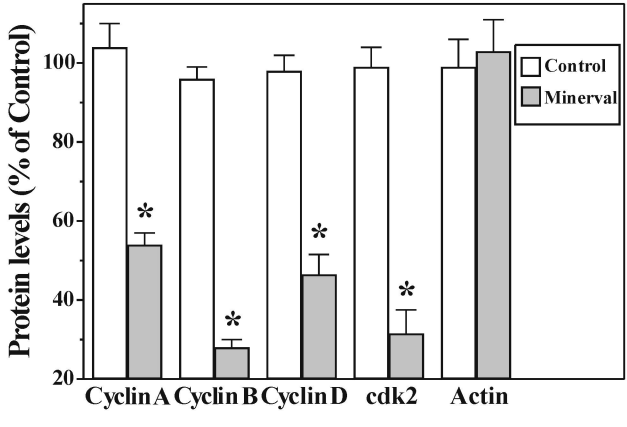
Protein levels (% of Control)
100
80
60
40
20
Control
Minerval
*
*
*
*
Cyclin A
Cyclin B
Cyclin D
cdk2
Actin

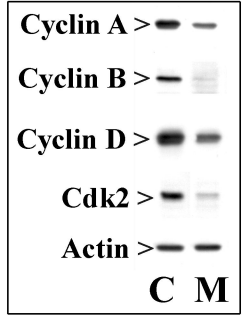
Cyclin A >
Cyclin B >
Cyclin D >
Cdk2 >
Actin >
C M

Figure 4

Molecular Pharmacology Fast Forward. Published on November 5, 2004 as DOI: 10.1124/mol.104.000778
This article has not been copyedited and formatted. The final version may differ from this version.

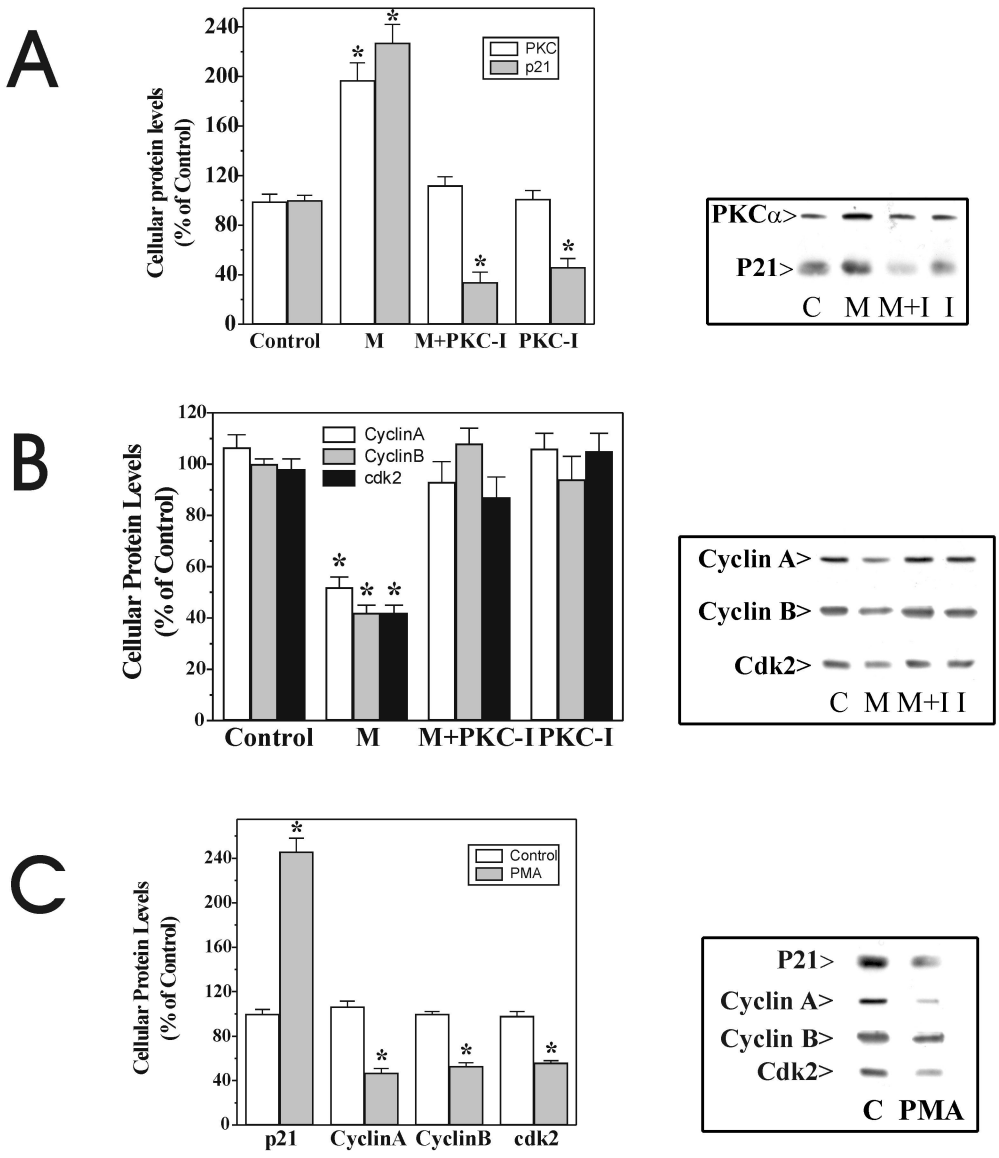

Figure 5